Corrosion prevention of AA2024-T3 aluminum alloy in acidic media using *Cydonia Vulgaris* leaves extract

Z.M. Awad,[1] A.N. Abd[1] and K.H. Hassan[2]*

[1]*University of Diyala, College of Science, Department of Chemistry, Diyala, Iraq*
[2]*Bilad Alrafidain University College, Diyala, 32001, Iraq*
**E-mail: dr.karimhan@bauc14.edu.iq*

Abstract

Aluminum is widely used as a material in automobiles, aviation, household appliances, containers, and electronic devices The resistance of aluminum against corrosion in aqueous media can be attributed to the rapid formation of oxide films on the surface. However, aluminum gets easily corroded in the presence of corrosive acids. Studies of the corrosion behavior of aluminum in different aggressive environments have continued to attract attention because of its important applications. The study of *Cydonia Vulgaris* leaves extract (CVL) as a corrosion inhibitor for AA2024-T3 aluminum alloy in 1 M H_3PO_4 acid solution using weight loss method was investigated at 25, 35, 45 and 55°C. The results revealed that CVL leaves in 1 M acidic environment decreased the corrosion at various concentrations considered. Higher inhibition efficiency for AA2024-T3 aluminum alloy of up to (94.58%) was produced at a higher levels of inhibitor concentrations and temperatures. The adsorption of CVL extracts was found to obey the Langmuir adsorption isotherm model. The values of the free energy of adsorption were more than –20 kJ/mol which is indicative of a mixed mode of physical and chemical adsorption. Activation enthalpy (ΔH^*) and activation entropy (ΔS^*) of AA2024-T3 aluminum alloy corrosion was found to be (48.7570 kJ·mol^{-1}), (–0.1782 kJ·K^{-1}) and (31.9920 kJ·mol^{-1}), (–0.1873 kJ·K^{-1}) in the absence and presence of the extract, respectively.

Received: October 26, 2022. Published: January 5, 2023 doi: 10.17675/2305-6894-2023-12-1-3

Keywords: *corrosion, AA2024-T3 aluminum alloy, adsorption, inhibitor efficiency, weight loss.*

Introduction

Corrosion is defined as the gradual destruction deterioration of metals or alloys by the chemical or electrochemical reaction with its environment [1]. Aluminum alloy AA2024-T3 (Al-Cu-Mg) is one of the best aluminium alloys which is used widely and applied as a structural material in the aviation industry, automotive industry and ship building. At present, conversion and paint coatings are used to protect Al alloys against corrosion [2]. Al alloys have many desirable properties such as high fluidity, light weight, low melting points, high thermal conductivity and good surface finish, these properties making aluminum alloys for using widely in casting [3]. Aluminum and most of the aluminum alloys have alloys have good corrosion resistance towards natural atmosphere and other environments because

aluminum surfaces are covered with a natural oxide film Al_2O_3. In the existence of aggressive environment, the protective layer can be locally destroyed and the corrosive attack takes place. Phosphoric acid is a major industrial chemical, which is widely used for acid cleaning and elector polishing of aluminum [4]. Even though dissolution rate of aluminum in phosphoric acid is lower, compared to the dissolution of it in hydrochloric or sulphuric acid, it does corrode aluminum and its alloys. Phosphoric acid is also used in pickling delicate, costly components and precision items where rerusting after pickling has to be avoided [5]. Corrosion inhibitors are those compounds when added to the corroding environment delays the phenomenon of corrosion. The inhibitors contain a number of heteroatoms like oxygen, sulphur, nitrogen etc. in their structure. The inhibitors control corrosion by simply blocking the active sites of the metal surface. The aim of using the inhibitor is to reduce the corrosion rate [6]. In the present work, extract of *Cydonia Vulgaris* leaves which are very common, available and cheap plants in Diyala governorate/Iraq was used and tested to control the corrosion of AA2024-T3 aluminum alloy in H_3PO_4 solution at different operating conditions. This natural material was used as a green and environmentally friendly that can substitute the artificial one.

Experimental

Chemicals

Phosphoric acid, methanol and acetone.

Materials

Aluminum alloy AA2024-T3. The composition of the AA2024-T3 aluminum alloy was determined by optical emission spectroscopy (OES) available in central organization for standardization and quality control as shown in Table 1.

Instruments and apparatus used in characterization

Analytical weighing balance, heating mantle, magnetic stirrer, water bath, desiccator. Optical Emission spectrometer (OES), Scanning Electron Microscope (SEM).

Preparation of test samples of AA2024-T3 aluminum alloy

The AA2024-T3 aluminum alloy samples of 1 cm thickness were cut into samples of 3x3 cm dimension with a hole drilled on its side for easy suspension into the corroding solution [7]. The samples were polished by using emery paper with different grades (220, 400, 600, 800, 1000, 1500 and 2000). Then the samples were rinsed with flow of tap water followed by distilled water. It was dried with hot air, and immersed in methanol and acetone, and then dried again and then stored in a desiccator over silica gel. The samples were weighted by a 4-digit electronic balance and the dimensions were measured by an electronic vernier. They were completely immersed in the corrosion solution and transferred to water bath.

Table 1. Composition of the AA2024-T3 aluminum alloy specimen (wt%).

AA2024-T3 aluminum alloy composition (wt%)	
Element	**Weight %**
Si	0.0655%
Fe	0.164%
Cu	4.04%
Mn	0.589%
Mg	1.37%
Cr	0.0040%
Ni	0.0024%
Zn	0.0808%
Ti	0.0297%
Ga	0.0074%
V	0.0081%
Al	99.19%

Weight-loss measurement

Specimens of AA2024-T3 aluminum alloy were used for weight loss measurements. The specimens cleaned and dried were completely immersed in 200 mL of 1 M H_3PO_4 solution with and without inhibitor for a period of 3 h, then the specimens were washed, dried by electric dryer and weighed using analytical balance. The weight loss was calculated using experiments conducted at different concentrations of inhibitor (1, 3, 5, 7, 9 and 11 mL/L) and at different temperatures (298.15, 308.15, 318.15 and 328.15 K).

Preparation of plant extract for corrosion inhibition studies

CVL leaves were collected from gardens, shade dried, and grinded to powder. The extract was prepared by refluxing 10 g of powder in 100 mL of 1 M H_3PO_4 acid for 3 h and kept overnight, then filtered and the filtrate was made up to 50 mL using the same acid and this was taken as stock solution. Portions with concentrations of 1, 3, 5, 7, 9 and 11 mL per liter of phosphoric acid solutions was used as a corrosion solution.

Results and Discussion

Weight loss measurement

From the change in weight of specimens, the corrosion rate was calculated using the following relationship [8].

$$C_{R_{\text{corr}}}(\text{mpy}) = \frac{534 \cdot W}{D \cdot T \cdot A} \quad (1)$$

where W is the weight loss in mg, D is the density of specimen (g/cm^3), A is the area of specimen in a square inch (note that 1 in^2=6.5416 cm^2), T is the exposure time in hours, mpy = mils per year. Corrosion rate was then used in the calculation of E_a, ΔS^*, and ΔH^*. The inhibition efficiency (%*IE*) was calculated using the following formula:

$$\%IE = \frac{W_{\text{uninh}} - W_{\text{inh}}}{W_{\text{uninh}}} \quad (2)$$

where W_{uninh}=weight loss without inhibitor, W_{inh}=weight loss with inhibitor [9].

The degree of surface coverage (θ) for different concentration of the inhibitor in acidic media have been evaluated from weight loss experiments using this equation:

$$\theta = \frac{IE}{100} \quad (3)$$

Corrosion rate and inhibitor efficiency were evaluated at different operating conditions. The results are presented in Table 2 through 28 test runs.

Effect of inhibitor concentration

Inhibition efficiency of AA2024-T3 aluminum alloy at different concentrations of Cydonia Vulgaris leaves extract in 1 M H_3PO_4 at room temperature is presented in Table 2. From the Table, it is clear that the corrosion rate decreases with an increase in inhibitor concentration. The corrosion inhibition enhances with the inhibitor concentration. This behavior is due to the fact that the adsorption and coverage of the inhibitor on the AA2024-T3 aluminum alloy surface increase with the inhibitor concentration. The high inhibitive performance of Cydonia Vulgaris suggests a higher bonding ability of inhibitor on AA2024-T3 aluminum alloy surface as in the corrosion of mild steel in 0.5 M HCl [10]. It is clear that corrosion rate increased with temperature and decreased with inhibitor concentration as shown in Figures 1 and 2.

Table 2. Corrosion rate (mpy) and inhibitor efficiency (%*IE*) and surface coverage (θ) as a function of temperature and concentration.

Time (3 h)					
No.	**C_{inh} (mL/L)**	**Temperature (°C)**	**C_R (mpy)**	**θ**	**%*IE***
1	Blank	25	205.878	0	0
2		35	371.924	0	0
3		45	791.824	0	0
4		55	1314.835	0	0

Time (3 h)					
No.	**C_{inh} (mL/L)**	**Temperature (°C)**	**C_R (mpy)**	**θ**	**%*IE***
5	1	25	89.289	0.5660	56.60
6		35	95.345	0.7456	74.56
7		45	112.448	0.8453	84.53
8		55	151.679	0.8848	88.48
9	3	25	73.979	0.6415	64.15
10		35	80.072	0.7874	78.74
11		45	91.128	0.8741	87.41
12		55	148.772	0.8877	88.77
13	5	25	58.980	0.7169	71.69
14		35	63.152	0.8327	83.27
15		45	79.662	0.8902	89.02
16		55	144.869	0.8907	89.07
17	7	25	39.627	0.8113	81.13
18		35	49.400	0.8675	86.75
19		45	65.769	0.9100	91.00
20		55	107.038	0.9192	91.92
21	9	25	30.150	0.8553	85.53
22		35	44.809	0.8815	88.15
23		45	55.200	0.9244	92.44
24		55	111.870	0.9399	93.99
25	11	25	20.115	0.9056	90.56
26		35	28.827	0.9233	92.33
27		45	44.667	0.9388	93.88
28		55	72.075	0.9458	94.58

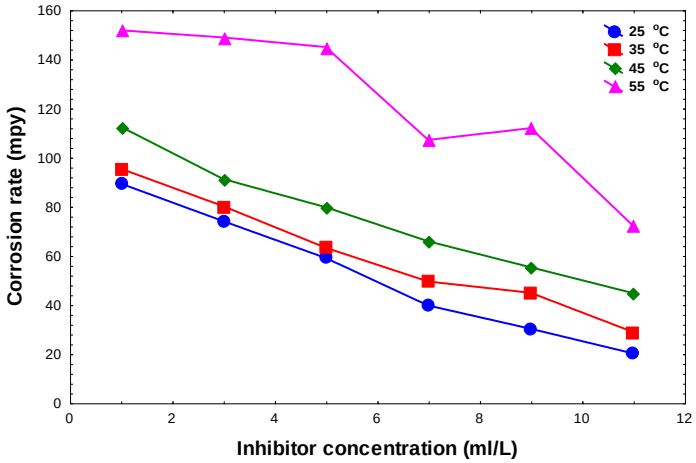

Figure 1. Effect of inhibitor (CVL extract) concentration on the corrosion rate of AA2024-T3 aluminum alloy immersed in 1 M H_3PO_4 for 3 h.

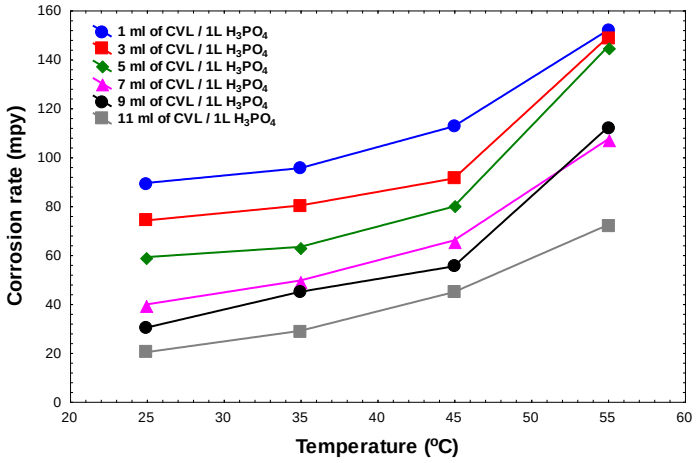

Figure 2. Effect of temperature on the corrosion rate of AA2024-T3 aluminum alloy in 1 M H_3PO_4 at at densis miller extract in 0.5 M different inhibitor (CVL extract) concentrations.

Effect of temperature and thermodynamic parameters calculations

The effect of temperature on the rate of corrosion of AA2024-T3 aluminum alloy in 1 M H_3PO_4 solution containing a different concentration from investigated inhibitors was tested by weight loss measurements over a temperature range from 25 to 55°C. The effect of increasing temperature on the corrosion rate and %*IE* obtained was from weight loss measurements. The results presented in Table 2 revealed that the rate of corrosion increases as the temperature increases and decreases as the concentration of these compounds increases. The activation energy E_a of the corrosion process was calculated [11] using Equation 4 from the slope of the plot of ln K against $1/T$ which is $-E_a/T$.

$$K = A\exp\left(-\frac{E_a}{RT}\right) \quad (4)$$

where K is the rate of corrosion, A is the Arrhenius constant, R is the gas constant and T is the absolute temperature. Figure 3 presents the Arrhenius plots in the presence and absence of inhibitor. Similar curves were obtained in the presence of other inhibitors concentrations, but not shown. E_a values determined from the slopes of these linear plots are shown in Table 3. The linear regression (R^2) is close to 1 which indicates that the corrosion of AA2024-T3 aluminum alloy in 1 M H_3PO_4 solution can be elucidated using the kinetic model. Table 3 also showed that the value of E_a inhibited solution is higher than that for uninhibited solution, suggesting that dissolution of AA2024-T3 aluminum alloy is slow in the presence of inhibitor and can be interpreted as due to chemical adsorption. It is known from Equation 4 that the higher E_a values lead to the lower corrosion rate. This is due to the formation of a film on AA2024-T3 aluminum alloy surface serving as an energy barrier for AA2024-T3 aluminum alloy corrosion. The enthalpy and entropy of activation (ΔH^*, ΔS^*) of the corrosion process were calculated from the transition state theory equation:

$$CR = \frac{RT}{Nh}\exp\left(\frac{\Delta S_{\text{act}}}{R}\right)\exp\left(\frac{\Delta H_{\text{act}}}{RT}\right) \tag{5}$$

where h is Planck's constant and N is Avogadro's number ($6.022 \cdot 10^{23}$). Equation 5 can be plotted as ln (CR/T) *versus* ($1/T$) to calculate the activation enthalpy and entropy from the slope $\left(-\frac{\Delta H_{\text{act}}}{R}\right)$ and intercept $\ln\left(\frac{R}{Nh}\right)+\left(\frac{\Delta S_{\text{act}}}{R}\right)$, respectively. Figure 4 presents the transition plots in the presence and absence of inhibitor. Similar curves were obtained in presence of the other inhibitors, but not shown and the data are given also in Table 3. The positive signs of ΔH^* reflect the endothermic nature of the AA2024-T3 aluminum alloy dissolution process. Large and negative values of ΔS^* imply that the activated complex in the rate-determining step represents an association rather than dissociation step, meaning that decrease in disordering takes place ongoing from reactants to the activated complex [12].

Table 3. Activation parameters.

***C* (mL/L)**	***E*$_a$ (kJ/mol)**	**Δ*H** (kJ/mol)**	**Δ*S** (kJ/mol·K)**
Blank	51.345	48.7570	–0.1782
1	13.879	11.5316	–0.1941
3	17.860	15.2627	–0.1928
5	23.508	20.9091	–0.1908
7	26.396	23.7992	–0.1900
9	33.481	30.8839	–0.1874
11	34.589	31.9920	–0.1873

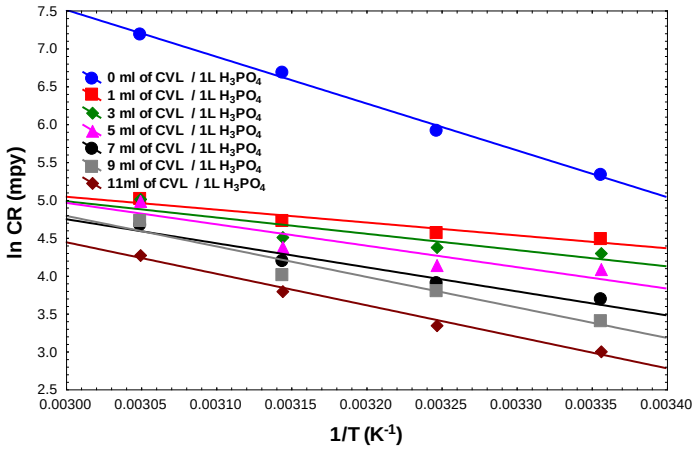

Figure 3. Arrhenius plots for AA2024-T3 aluminum alloy corrosion rates in 1 M H_3PO_4 in the absence and in the presence of different concentrations of CVL.

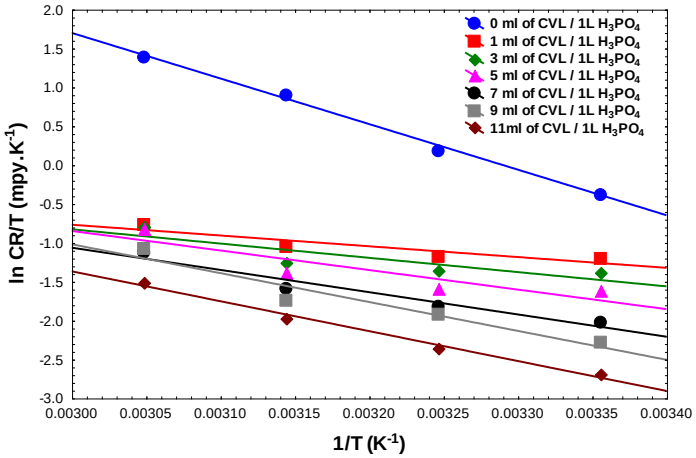

Figure 4. Transition state plots for AA2024-T3 aluminum alloy corrosion rates (1 M H_3PO_4) in the absence and in the presence of different concentrations of CVL.

Adsorption isotherms

Organic compounds as green corrosion inhibitors decrease the corrosion of metal through the adsorption on the metallic surface followed by forming a protective layer. In order to understand the mechanism of corrosion inhibition, the adsorption behavior of the adsorbate on the AA2024-T3 aluminum alloy surface must be known. The information on the interaction between the inhibitor molecules and the metal surface can be provided by adsorption isotherm. The degree of surface coverage ($\theta = \%IE/100$) for different concentrations of inhibitor was evaluated from weight loss measurements. Three models were suggested to study the kinetics of adsorption of CVL on metal surface. Langmuir adsorption isotherm (Equation 6), Freundlich adsorption isotherm (Equation 7), and Temkin adsorption isotherm (Equation 8) were tried. It was found that the data best fit the Langmuir adsorption isotherm.

$$\frac{C}{\theta} = \frac{1}{K_{ads}} + C \tag{6}$$

$$\theta = K_{ads} C^{n} \tag{7}$$

$$\exp(-2a\theta) = K_{ads} C \tag{8}$$

where θ is the degree of surface coverage, C is the concentration of the inhibitor, K_{ads} is the adsorptive equilibrium constant, and a is the molecular interaction parameters Equation 6, Equation 7 and Equation 8 can be plotted as shown in Figure 5, Figure 6, and Figure 7, respectively. The Gibbs standard free energy of adsorption of the organic inhibitor was estimated by means of Equation 9:

$$K_{ads} = \frac{1}{1000} \exp\left(\frac{-\Delta G^{0}_{ads}}{RT}\right) \tag{9}$$

where $R = 8.314$ J·mol^{-1} is the universal gas constant, 1000 is the concentration of water in the corrodent solution (mL/L) while T is the absolute temperature in Kelvin. From Table 4, the ΔG^{0}_{ads} values are negative in at all models used and lie in the range of –16.354 to –22.895 kJ·mol^{-1}. It is clearly observed that the acid concentration increases the values of ΔG^{0}_{ads} which revealed that the most efficient inhibitor shows more negative value, ΔG^{0}_{ads} with a decrease in the inhibition efficiency and increase in acid concentration with a physical adsorption. This suggests that a strongly adsorbed on the metal surface. Generally, values of ΔG^{0}_{ads} more negative than –20 kJ·mol^{-1} indicate physical adsorption while those more negative than –40 kJ·mol^{-1} indicate chemical adsorption. The values of ΔG^{0}_{ads} obtained in this experiment being less negative than –20 kJ·mol^{-1} also support physisorption process [13–15].

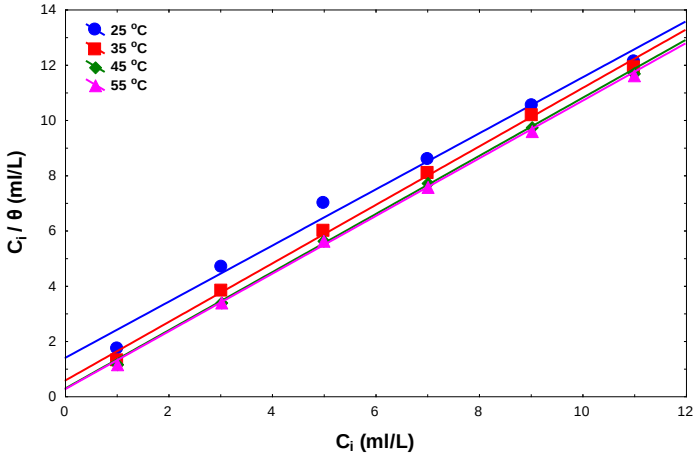

Figure 5. Langmuir adsorption isotherm of AA2024-T3 aluminum alloy in 1 M H_3PO_4 under different conditions.

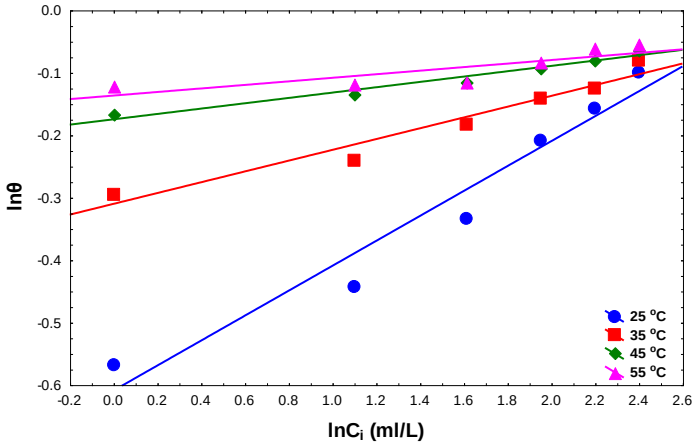

Figure 6. Freundlich adsorption isotherm of AA2024-T3 aluminum alloy in 1 M H_3PO_4 under different conditions.

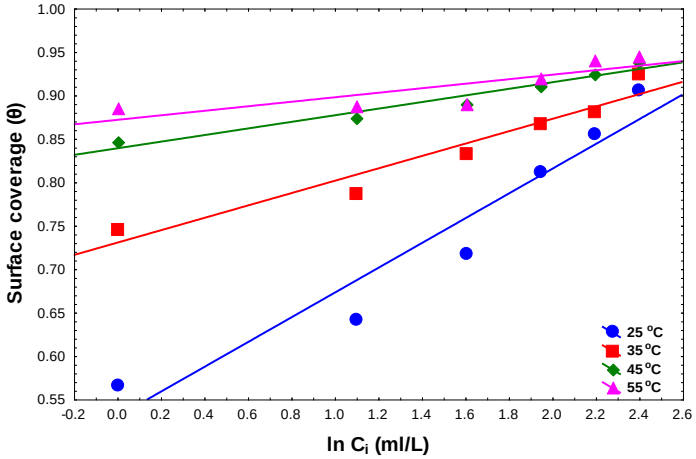

Figure 7. Temkin adsorption isotherm of AA2024-T3 aluminum alloy in 1 M H_3PO_4 under different conditions.

Table 4. Adsorption parameters for corrosion of AA2024-T3 aluminium alloy.

***T*, K**	**Langmuir adsorption isotherm**			**Freundlich adsorption isotherm**			**Temkin adsorption isotherm**		
	K_{ads} **(ml/L)**	ΔG^0_{ads} **(ml/L)**	R^2	K_{ads} **(ml/L)**	***n***	R^2	K_{ads} **(ml/L)**	***a***	R^2
298.15	6.6010	–16.354	0.9876	0.4951	0.199	0.9519	0.5297	0.1426	0.9249
308.15	7.5282	–19.277	09973	1.1695	0.086	0.9494	0.7299	0.0712	0.9360
318.15	8.2964	–21.934	0.9994	1.7423	0.042	0.9607	0.8385	0.038	0.9544
328.15	8.3958	–22.895	0.9992	1.9870	0.028	0.7043	0.8713	0.026	0.7015

Surface analysis using SEM

Scanning electron microscopy (SEM) was used to examine the surface of AA2024-T3 aluminum alloy species. The AA2024-T3 aluminum alloy species before and after immersion in the absence and presence of the CVL plant leaves extract for a period of 3 h at 55°C were taken out. The SEM micrographs of the examined surfaces are shown in Figure 8 (a, b, c) for AA2024-T3 aluminum alloy coupons respectively. The SEM micrograph of the polished AA2024-T3 aluminum alloy metal is shown in surface given in Figure 8(a) was smooth in the absence of any corrosion products but in Figure 8(b) they were damaged when immersed in 1 M H_3PO_4. This occurred as a result of the attack of the corrosive solution in the absence of the inhibitor. On addition of the inhibitor, there was an improvement in the metal surface as shown in Figure 8(c) for AA2024-T3 aluminum alloy coupons respectively. This improvement in surface morphology was due to the formation a good protective film which was responsible for the inhibition of corrosion [16].

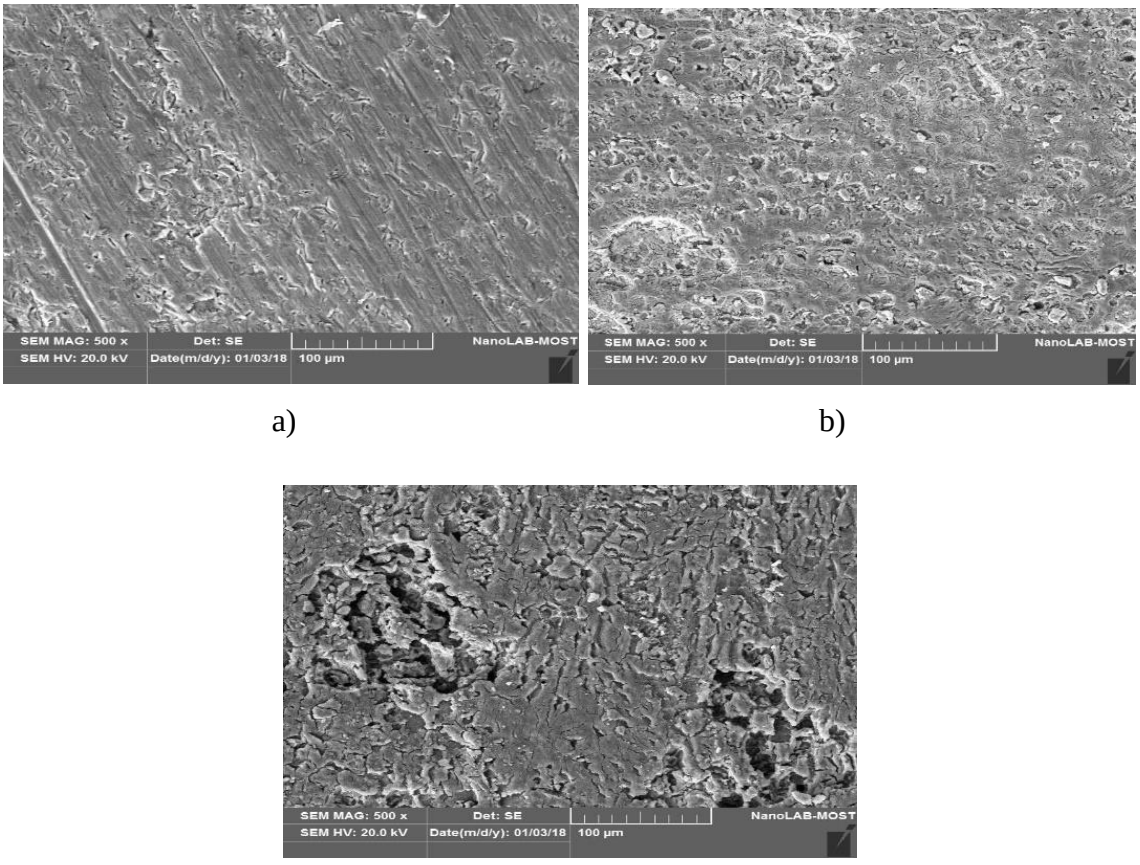

Figure 8. SEM images of AA2024-T3 aluminum alloy surface at 55°C for 3 h: (a) AA2024-T3 aluminum alloy before immersion in corrosion solution; (b) after immersion in 1 M H_3PO_4; (c) after immersion in 1 M H_3PO_4 in presence of the CVL inhibitor.

Conclusions

From the results obtained it is evident that CVL in 1 M H_3PO_4 acidic media decreased the corrosion at various concentrations studied where a higher inhibition efficiency for AA2024-T3 aluminum alloy of up to 94.58% was produced at a higher levels of inhibitor concentrations and temperatures. Adsorption isotherms investigation indicated that the adsorption process obeys the Langmuir adsorption isotherm model. The values of the free energy of adsorption were higher than –20 kJ/mol which is indicative of a mixed mode of physical and chemical adsorption. Finally, the activation enthalpy (ΔH^*) and activation entropy (ΔS^*) of AA2024-T3 aluminum alloy corrosion were found to be (48.7570 $kJ \cdot mol^{-1}$), (–0.1782 $kJ \cdot K^{-1}$) and (31.9920 $kJ \cdot mol^{-1}$), (–0.1873 $kJ \cdot K^{-1}$) in the absence and in the presence of the extract, respectively.

Acknowledgements

The authors would like to thank the Department of Chemistry–College of Science–University of Diyala for continuous support and facilities.

References

1. T. Lakshmikandhan and C. Boss, Development of inhibition efficiency, thermodynamic and kinetic properties of alanine on aluminum corrosion in hydrochloric acid, *Int. J. Pure Appl. Math*., 2018, **119**, no. 12, 6047–6063.
2. A.M. Semiletov, Protection of aluminum alloys from atmospheric corrosion by thin films of inhibitors, *Int. J. Corros. Scale Inhib*., 2017, **6**, no. 4, 449–462. doi: 10.17675/2305-6894-2017-6-4-5
3. A.M. Al-Uqaily, Effect of quenching media on corrosion resistance of Al-Si-Mg alloy, *Al-Qadisiyah Journal of Pure Science*, 2014, **19**, no. 1, 1–14.
4. D. Prabhu and P. Rao, Garcinia indica as an environmentally safe corrosion inhibitor for aluminum in 0.5 M phosphoric acid, *Int. J. Corros*., 2013, **2**, 1–12.
5. Prabhu D. and Rao. P., Studies of corrosion of aluminium and 6063 aluminium alloy in phosphoric acid medium, *Int. J. Chem. Tech. Research*, 2013, **5**, no. 6, 2690–2705.
6. M. Anbarasi and K. Suruthi, Chrysanthemum Flower Extract as a Green Inhibitor for Aluminium Corrosion in Alkaline Medium, *Int. J. Chem. Tech. Research*, 2018, **11**, no. 7, 37–44.
7. P.I. Okek, O.G. Maduka, R.U. Emeronye, C.O. Akalezie, Mughele K. Achinihu I.O. and Azubuike N.E., Corrosion inhibition efficacy of Cninodosculus chayamansa extracts on aluminium metal in acidic and alkaline media, *Int. J. Sci. Technol*., 2015, **3**, no. 3, 227–234.
8. M.E. Al-Dokheily, H.M. Kredy and R.N. Al-Jabery, Inhibition of copper corrosion in H_2SO_4, NaCl and NaOH solutions by citrullus colocynthis fruits extract, *J. Nat. Sci. Res*., 2014, **4**, 60–73.

9. R.T. Vashi and N.I. Prajapati, Corrosion inhibition of aluminium in Hydrochloric acid using Bacopa monnieri leaves extract as green inhibitor, *Int. J. Chem. Tech. Research*, 2017, **10**, no. 15, 221–231.
10. A.M. Preetha and F.R. Selvarani, Corrosion inhibition of mild steel using aloe barbedensis miller skin extract in 0.5 M HCL, *Int. J. Adv. Res*., 2017, **5**, no. 3, 1457–1467.
11. A.A. Khadom, A.F. Hassan and B.M. Abod, Evaluation of environmentally friendly inhibitor for galvanic corrosion of steel–copper couple in petroleum waste water, *Process Saf. Environ. Prot*., 2015, **98**, 93–101.
12. A.S. Fouda, M.A. Elmorsi and A. Elmekkawy, Eco-friendly Chalcones derivatives as corrosion inhibitors for carbon steel in hydrochloric acid solution, *Afr. J. Pure Appl. Chem*., 2013, **7**, no. 10, 337–349.
13. G.I. Udom, G.A. Cookey and A.A. Abia, The Effect of acanthus montanus leaves extract on corrosion of aluminium in hydrochloric acid medium, *Curr. J. Appl. Sci. Technol*., 2017, **25**, no. 2, 1–11.
14. F.M. Bin Yehmed, A.M. Abdullah, Z. Zainal and R.M. Zawawi, Green Coffee Bean Extract as a Green Corrosion Inhibitor for Aluminium in Artificial Acid Rain Medium, *Int. J. Appl. Environ. Sci*., 2018, **13**, no. 2, 171–183.
15. P.S. Desai, Calotropis gigantea leaves ark used as corrosion inhibitor for aluminium in hydrochloric acid, *Der Pharma Chem*., 2018, **10**, no. 1, 7–12.
16. M. Anbarasi and K.S. Suruthi, Chrysanthemum flower extract as a green inhibitor for aluminum corrosion in alkaline medium, *Int. J. Chem. Tech. Research*, 2017, **11**, no. 7, 37–44.

♦ ♦ ♦